

Electronic Properties of Single-Walled Carbon Nanotube Networks

Elena Bekyarova, Mikhail E. Itkis, Nelson Cabrera, Bin Zhao, Aiping Yu, Junbo Gao, and Robert C. Haddon*

Contribution from the Center for Nanoscale Science and Engineering, and Departments of Chemistry and Chemical & Environmental Engineering, University of California, Riverside, California 92521

Received November 14, 2004; E-mail: haddon@ucr.edu

Abstract: We present a study on the electronic behavior of films of as-prepared and purified single-walled carbon nanotubes (SWNTs) and demonstrate the important role that chemical functionalization plays in modifying their electronic properties, which in turn throws further light on the mechanism of action of SWNT-based sensors. Films of electric arc SWNTs were prepared by spraying, and optical spectroscopy was used to measure the effective film thickness. The room-temperature conductivities ($\hat{\sigma}_{\text{RT}}$) of thin films deposited from as-prepared and purified SWNTs are in the range $\hat{\sigma}_{\text{RT}} \sim 250\text{--}400\text{ S/cm}$, and the nonmetallic temperature dependence of the conductivity indicates the presence of tunneling barriers, which dominate the film conductivity. Chemical functionalization of SWNTs with octadecylamine (ODA) and poly(*m*-aminobenzenesulfonic acid) (PABS) significantly decreases the conductivity; $\hat{\sigma}_{\text{RT}} \sim 3$ and 0.3 S/cm for SWNT-ODA and SWNT-PABS, respectively.

Introduction

As a result of their quasi 1-D structure and unique electronic properties, single-walled carbon nanotubes (SWNTs) are appealing candidates for applications within molecular electronics;¹ because they can be metals or semiconductors, SWNTs provide the necessary building blocks for electronic circuits. SWNTs afford new opportunities for chip miniaturization, which can dramatically improve the scaling prospects for the semiconductor technologies. Techniques have been reported for the fabrication of devices based on individual SWNTs, including field effect transistors,^{2,3} sensors,⁴ and rectifiers.⁵ Individual carbon nanotube-based devices already outperform conventional silicon FETs in certain figures of merit, such as current carrying capacity,^{1,6} room-temperature effective mobility resulting from ballistic transport,⁷ and degree of miniaturization.¹ However, the assembly and connection of individual SWNTs to metal contacts remain a challenge and, taken together with the absence of highly purified SWNTs of specific chirality and electronic structure, currently impede the practical application of electronic devices based on individual SWNTs.

Carbon nanotube films have been explored as an alternative configuration for electronic devices,^{8–14} because such films are


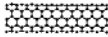
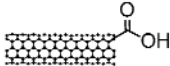
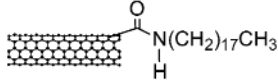
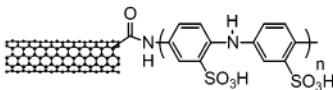
readily fabricated and give reproducible characteristics. The feasibility of using SWNT networks as diodes,¹⁵ transistors,¹⁴ field effect transistors (FET),^{8,9,13} and chemical sensors^{16,17} has already been demonstrated. Thin films of random networks of SWNTs have been shown to exhibit p-type semiconducting behavior and can operate as the conducting channel of an FET.^{8,9} Although the performance is inferior to individual nanotube devices, the network devices have a field-effect mobility about an order of magnitude larger than that of materials typically used in thin-film transistors.⁹ Additionally, because of their optical transparency, SWNT films have been suggested for conductive coatings as an alternative to indium tin oxide (ITO).^{13,18}

The optimization of SWNT networks and the detailed understanding of their electronic properties are expected to offer considerable scope for the development of carbon nanotube-based electronics and to have important implications for sensor devices.^{16,17} We present an analysis of the conductivity of thin

- (1) Avouris, P. *Acc. Chem. Res.* **2002**, *35*, 1026–1034.
- (2) Tans, S. J.; Verschueren, R. M.; Dekker, C. *Nature* **1998**, *393*, 49–52.
- (3) Martel, R.; Schmidt, T.; Shea, H. R.; Hertel, T.; Avouris, P. *Appl. Phys. Lett.* **1998**, *73*, 2447–2449.
- (4) Kong, J.; Franklin, N. R.; Zhou, C.; Chapline, M. G.; Peng, S.; Cho, K.; Dai, H. *Science* **2000**, *287*, 622–625.
- (5) Collins, P. G.; Zettl, A.; Bando, H.; Thess, A.; Smalley, R. E. *Science* **1997**, *278*, 100–102.
- (6) Frank, S.; Poncharal, P.; Wang, Z. L.; de Heer, W. A. *Science* **1998**, *280*, 1744–1746.
- (7) Durkop, T.; Getty, S. A.; Cobas, E.; Fuhrer, M. S. *Nano Lett.* **2004**, *4*, 35–39.

- (8) Bradley, K.; Gabriel, J.-C. P.; Gruner, G. *Nano Lett.* **2003**, *3*, 1353–1355.
- (9) Snow, E. S.; Novak, J. P.; Campbell, P. M.; Park, D. *Appl. Phys. Lett.* **2003**, *82*, 2145–2147.
- (10) Lay, M. D.; Novak, J. P.; Snow, E. S. *Nano Lett.* **2004**, *4*, 603–606.
- (11) Stadermann, M.; Papadakis, S. J.; Falvo, M. R.; Novak, J.; Snow, E.; Fu, Q.; Liu, J.; Fridman, Y.; Boland, J. J.; Superfine, R.; Washburn, S. *Phys. Rev. B* **2004**, *69*, 201401–201403.
- (12) Hu, L.; Hecht, D. S.; Gruner, G. *Nano Lett.* **2004**, *4*, 2513–2517.
- (13) Wu, Z.; Chen, Z.; Du, X.; Logan, J. M.; Sippel, J.; Nikolou, M.; Kamaras, K.; Reynolds, J. R.; Tanner, D. B.; Hebard, A. F.; Rinzler, A. G. *Science* **2004**, *305*, 1273–1276.
- (14) Meitl, M. A.; Zhou, Y.; Gaur, A.; Jeon, S.; Usrey, M. L.; Strano, M. S.; Rogers, J. A. *Nano Lett.* **2004**, *4*, 1643–1647.
- (15) Zhou, Y.; Gaur, A.; Hur, S.-H.; Kocabas, C.; Meitl, M. A.; Shim, M.; Rogers, J. A. *Nano Lett.* **2004**, *4*, 2031–2035.
- (16) Novak, J. P.; Snow, E. S.; Houser, E. J.; Park, D.; Stepnovski, J. L.; McGill, R. A. *Appl. Phys. Lett.* **2003**, *83*, 4026–4028.
- (17) Bekyarova, E.; Davis, M.; Burch, T.; Itkis, M. E.; Zhao, B.; Sunshine, S.; Haddon, R. C. *J. Phys. Chem. B* **2004**, *108*, 19717–19720.
- (18) Saran, N.; Parikh, K.; Suh, D.-S.; Munoz, E.; Kolla, H.; Manohar, S. K. *J. Am. Chem. Soc.* **2004**, *126*, 4462–4463.

Table 1. Purity and Chemical Characteristics of the SWNT Materials

Material	Relative carbonaceous SWNT purity, ^a %	Metal content, wt%	Structure
AP-SWNTs	46	31	
P2-SWNTs	89	10	
P3-SWNTs	94	10	
SWNT-ODA (50% SWNT loading)	90	5	
SWNT-PABS (35% SWNT loading)	90	3	

^a The carbonaceous purity was estimated against reference sample R2.²¹

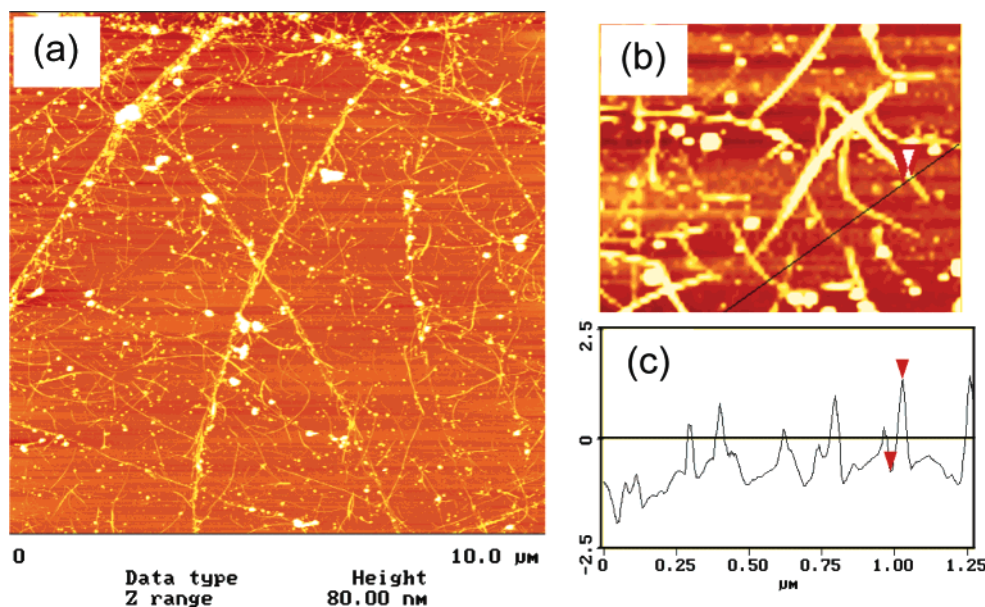


Figure 1. (a, b) AFM images of a SWNT network formed on a mica substrate by spraying. (c) Cross-section of the SWNT bundles imaged in (b); red arrows indicate a height corresponding to a bundle diameter of 2.1 nm. The images were recorded with a Nanoscope3 MultiMode atomic force microscope (Digital Instruments, Santa Barbara).

films of as-prepared and purified SWNT networks, which allows us to propose a simple model for their electronic response and to demonstrate the important role that chemical functionalization plays in modifying the electronic properties of carbon nanotube networks.

Experimental Section

Materials. In this study we used SWNTs prepared by the electric arc discharge method.^{19,20} As-prepared (AP) SWNTs, purified SWNTs (P2 and P3), and octadecylamine (ODA) functionalized and poly(*m*-aminobenzenesulfonic acid) (PABS) functionalized SWNTs were

provided by Carbon Solutions, Inc. (www.carbonsolution.com). General characteristics of the materials are given in Table 1.

Preparation of SWNT Films. The films were prepared by spraying dimethylformamide (DMF) dispersions of SWNTs on glass substrates with patterned silver electrodes (20 nm Cr/100 nm Ag). To ensure a high degree of nanotube dispersion, we used standard solutions with a concentration of 0.02 mg/mL, which were prepared by ultrasonication for 1 h in a bath sonicator (Aquasonic HT50). Figure 1 shows a typical AFM image of a SWNT network formed by spraying on a mica substrate. In the case of very thin films, optical microscopy confirmed the formation of homogeneous films that were free of nanotube aggregates. However the degree of aggregation increased with the film thickness.

Films of octadecylamine (ODA) functionalized SWNTs (SWNT-ODA) were prepared from THF solutions, whereas aqueous solutions were used to deposit poly(*m*-aminobenzenesulfonic acid) (PABS) functionalized SWNTs (SWNT-PABS).

- (19) Journet, C.; Maser, W. K.; Bernier, P.; Loiseau, A.; Lamy de la Chapelle, M.; Lefrant, S.; Deniard, P.; Lee, R.; Fischer, J. E. *Nature* **1997**, *388*, 756–758.
- (20) Itkis, M. E.; Perea, D.; Niyogi, S.; Love, J.; Tang, J.; Yu, A.; Kang, C.; Jung, R.; Haddon, R. C. *J. Phys. Chem. B* **2004**, *108*, 12770–12775.

Film Characterization. The near-IR (NIR) spectra were recorded on a Varian CARY 500 UV- vis- NIR spectrophotometer. The film thickness was calculated from the areal absorbance of the second semiconducting interband transition, S_{22} (see below). The I- V curves were measured at room temperature in ambient air with a Keithley 236 source-measure unit controlled by custom LabVIEW software. Both four- and two-probe dc measurements were conducted, and the contact resistance was found to be negligible in the voltage range from - 5 to 5 V, and the conductivities reported below are obtained from two-probe measurements. The temperature dependence of resistivity was measured in a custom-made helium variable-temperature probe using a Lake Shore 340 temperature controller.

Results and Discussion

Electronic Properties of As-Prepared and Purified SWNT Networks. A wide range of conductivities have been reported for SWNT films: from 12.5 S/cm¹⁴ to $\approx 10\,000$ S/cm.²² Relatively transparent films with a conductivity of ≈ 6700 S/cm have been prepared from SWNTs grown by pulsed laser vaporization and purified with nitric acid.¹³ Films of HiPco SWNTs prepared from oleum dispersions were reported to give $\sigma_{RT} \approx 900\text{--}1300$ S/cm.²³ The conductivity of SWNT mats is reported to be in the range 200– 500 S/cm.^{24– 27} Films of SWNTs obtained by laser ablation exhibit a conductivity of 50 S/cm.¹⁸ In many cases, the conductivities of SWNT films are far below the experimentally observed values of 10 000– 30 000 S/cm for the axial conductivity of a SWNT rope.²⁸ The lower conductivities observed for the SWNT films are presumably due to the lack of alignment and the existence of high resistances and Schottky barriers at the intertube junctions. The inhomogeneous distribution of SWNT constituents with respect to length, diameter, and chirality further complicates the electronic properties of the films.

To study the electronic properties of networks of as-prepared and purified electric arc SWNTs, films of various thicknesses were prepared on glass substrates with silver electrodes, and an effective film thickness was estimated from the NIR absorbance. Previous studies have demonstrated the applicability of Beer's law to carbon nanotube materials, which allowed the estimation of their extinction coefficient, ϵ .^{29,30} The optical film thickness was obtained from the areal absorbance of the second semiconducting interband transition (S_{22}), which occurs in the spectral range 7750– 11 750 cm⁻¹ for electric arc SWNTs, and the effective extinction coefficient (ϵ) of the material (Supporting Information). The effective extinction coefficients used in the calculations are 342 L, mol⁻¹, cm⁻¹ for AP-SWNTs, 408 L, mol⁻¹, cm⁻¹ for P2-SWNTs, and 277 L, mol⁻¹, cm⁻¹ for P3-

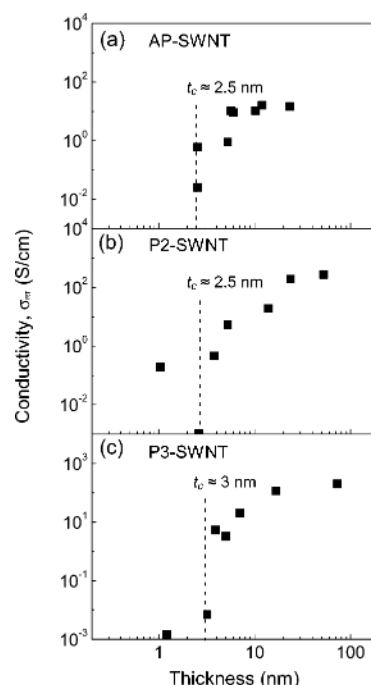


Figure 2. Room-temperature conductivity of (a) AP-SWNT, (b) P2-SWNTs, and (c) P3-SWNTs as a function of film thickness, where t_c indicates the abrupt change in conductivity.

SWNTs.²⁹ The choice of the second semiconducting interband transitions for calculation of the optical thickness is based on previous studies showing that these transitions are less affected by doping during chemical purification than the first semiconducting interband transitions (S_{11}).^{21,31} Experimental densities were obtained by immersing SWNTs in liquids of various densities (modified density gradient method).³² The densities of the nonfunctionalized SWNTs were found to be in the range 1.53– 1.59, and we adopted a density of 1.59 g, cm⁻³ for estimating the effective film thickness. In the case of the functionalized materials we obtained values of $d \approx 1.45$ g, cm⁻³ for PABS-SWNTs and $d \approx 1.37$ g, cm⁻³ for SWNT-ODA.

To check the accuracy of the thickness estimation from the absorption experiments, we used two other techniques to measure the film thickness (see Supporting Information). We recorded AFM images at the film edges, to compare the measurement of film thicknesses by absorption spectroscopy and AFM.^{13,18} The optical characterization technique has the clear advantage that it is unambiguous and rapidly accomplished. As expected, we find the film thickness obtained from AFM to be consistently greater than the value measured by optical spectroscopy ($\approx 15\%$). As a further check for errors in the thickness estimation due to reflectance and scattering, we redispersed some of the films in DMF and estimated the thickness of the films by solution spectroscopy; the values obtained from the film measurements are consistent with those obtained from diluted dispersions, in which scattering is not significant.³³

The conductivities of films of as-prepared (AP-SWNTs) and purified (P2- and P3-) SWNTs are shown in Figure 2. The three SWNT materials show similar behavior. It may be seen that

- (21) Itkis, M. E.; Perea, D.; Niyogi, S.; Rickard, S.; Hamon, M.; Hu, H.; Zhao, B.; Haddon, R. C. *Nano Lett.* **2003**, *3*, 309– 314.
- (22) Hone, J.; Llaguno, M. C.; Nemes, N. M.; Johnson, A. T.; Fischer, J. E.; Walters, D. A.; Casavant, M. J.; Schmidt, J.; Smalley, R. E. *Appl. Phys. Lett.* **2000**, *77*, 666– 668.
- (23) Sreekumar, T. V.; Liu, T.; Kumar, S.; Ericson, L. M.; Hauge, R. H.; Smalley, R. E. *Chem. Mater.* **2003**, *15*, 175– 178.
- (24) Fischer, J. E.; Dai, H.; Thess, A.; Lee, R.; Hanjani, N. M.; Dehaas, D. L.; Smalley, R. E. *Phys. Rev. B* **1997**, *55*, R4921– R4924.
- (25) Kim, G. T.; Choi, E. S.; Kim, D. C.; Suh, D. S.; Park, Y. W. *Phys. Rev. B* **1998**, *58*, 16064– 16069.
- (26) Kaiser, A. B.; Dusberg, G.; Roth, S. *Phys. Rev. B* **1998**, *57*, 1418– 1421.
- (27) Bozhko, A. D.; Sklovsky, D. E.; Nalimova, V. A.; Rinzler, A. G.; Smalley, R. E.; Fischer, J. E. *Appl. Phys. A* **1998**, *67*, 75– 77.
- (28) Thess, A.; Lee, R.; Nikolaev, P.; Dai, H.; Petit, P.; Robert, J.; Xu, C.; Lee, Y. H.; Kim, S. G.; Rinzler, A. G.; Colbert, D. T.; Scuseria, G. E.; Tomanek, D.; Fischer, J. E.; Smalley, R. E. *Science* **1996**, *273*, 483– 487.
- (29) Zhao, B.; Itkis, M. E.; Niyogi, S.; Hu, H.; Zhang, J.; Haddon, R. C. *J. Phys. Chem. B* **2004**, *108*, 8136– 8141.
- (30) Zhao, B.; Itkis, M. E.; Niyogi, S.; Hu, H.; Perea, D.; Haddon, R. C. *J. Nanosci. Nanotech.* **2004**, *4*, 995– 1004.

- (31) Itkis, M. E.; Niyogi, S.; Meng, M.; Hamon, M.; Hu, H.; Haddon, R. C. *Nano Lett.* **2002**, *2*, 155– 159.
- (32) Buchanan, F. J.; White, J. R.; Sim, B.; Downes, S. *J. Mater. Sci.: Mater. Med.* **2001**, *12*, 29– 37.
- (33) Itkis, M. E.; Perea, D.; Jung, R.; Niyogi, S.; Haddon, R. C. *J. Am. Chem. Soc.* **2005**, *127*, 3439– 3448.

the conductivities of the individual films vary by about 4 orders of magnitude as the thickness increases from 1 to 100 nm and that there is a pronounced change in the value of the conductivity in the vicinity of a film thickness of 3 nm. As more SWNTs are deposited, the conductivity continues to increase rapidly until a film thickness of ≈ 50 nm is reached. Beyond this point the conductivity is relatively invariant to further increases of the film thickness. The room-temperature conductivity of AP-SWNT films reaches $\hat{\sigma}_{\text{RT}} \approx 250$ S/cm for films of thickness greater than 50 nm, and the conductivity of thick films of purified P2-SWNTs is similar to that of AP-SWNTs ($\hat{\sigma}_{\text{RT}} \approx 230$ S/cm), whereas the purified P3-SWNTs show slightly higher conductivity, $\hat{\sigma}_{\text{RT}} \approx 400$ S/cm.

The conductivities show a strong dependence on the film thickness (t), and in all cases there is a sharp increase in the conductivity in the vicinity of $t \approx 2-3$ nm; such behavior is characteristic of a percolating network. Near the percolation threshold (p_c) the conductivity ($\hat{\sigma}$) is expected to be related to the concentration of conducting channels (p) by a universal power law of the form $\hat{\sigma} \propto (p - p_c)^R$.^{34,35} We found that our conductivity data could be fit directly to the film thickness, according to eq 1:

$$\hat{\sigma}_{\text{RT}} \propto (t - t_c)^R \quad (1)$$

where t and t_c are the film thickness and critical thickness (percolation threshold), and R is a critical exponent. In the SWNT networks the overall resistance is dominated by the tube-tube or bundle-bundle contact resistance, and thus the concentration of conducting channels is expected to scale as the concentration of low resistance intertube junctions; this microscopic view of the conductivity in these films is supported by the temperature dependence of the conductivity discussed below. The concentration of these intertube junctions increases as more nanotubes are deposited and the film thickness increases up to the point that the conductivity saturates ($t \approx 50$ nm); at this point the film morphology is such that the conductivity is no longer a function of the film roughness. In this respect, we assume that the concentration of conducting nanotube-nanotube contacts in our films is proportional to the film thickness. The fits of eq 1 to our data are shown in Figure 3 and confirm the applicability of percolation theory to the SWNT networks. The critical thickness obtained from the unconstrained fits ($t_c \approx 3$ nm) reproduces the break in the conductivities discussed above (Figure 2). This value is very close to the average diameter of a bundle of SWNTs ($d \approx 4-6$ nm), which indicates that the deposition of a single layer of nanotube bundles is sufficient to give conducting channels. In support of this interpretation, we find that the $I-V$ curves are nonlinear below the percolation threshold, which we suggest is characteristic of tunneling between isolated clusters.

The critical exponents, R , obtained from fitting the experimental data are in the range 0.8-1.0; the critical exponent provides an index of the system dimensionality, and theoretical values of 1.3 and 1.94 have been predicted for ideal 2-D and 3-D systems, respectively.³⁴ Thus, it is reasonable to assume that near the percolation threshold the SWNT networks behave as quasi 2-D systems, which is consistent with the length

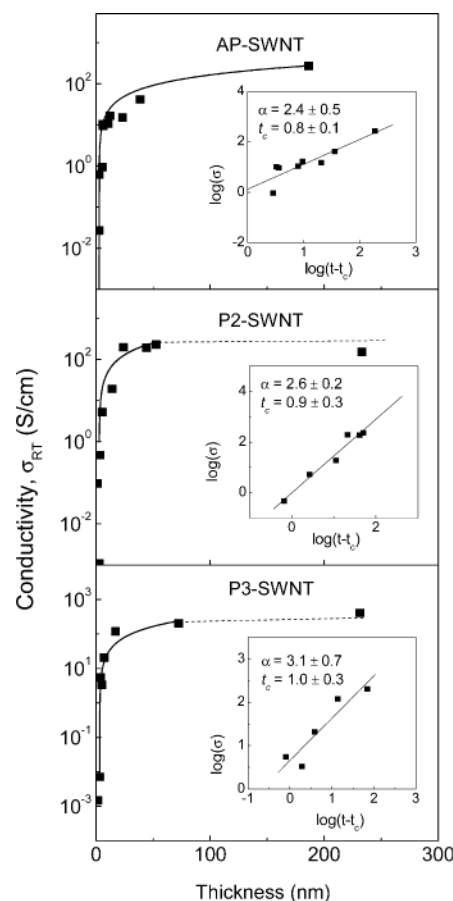


Figure 3. Conductivity of (a) AP-SWNT, (b) P2-SWNT, and (c) P3-SWNT films as a function of film thickness. The solid lines are fits of the experimental data to the power scaling equation $\hat{\sigma}_{\text{RT}} \propto (t - t_c)^R$. The insets show the conductivity, $\hat{\sigma}_{\text{RT}}$, as a function of $(t - t_c)$ on a logarithmic scale.

scales: the film thickness is much smaller than the average nanotube length (1 μ m). Typical SEM images of SWNT networks below and above the percolation threshold are given in Figure 4. Below the critical thickness of 2 nm, the images show the formation of clusters of interconnected nanotubes that remain isolated from each other and therefore do not form a conducting channel. Above the percolation threshold, a dense network of interconnected tubes representing multiple conducting channels is formed.

The experimentally measured conductivities of the SWNT networks are significantly lower than the conductivity of a SWNT rope (axial conductivity $\approx 10\,000-30\,000$ S/cm),²⁴ which suggests that the resistance of the networks is dominated by the resistance of the intertube junctions.^{11,12} Experimental studies of junctions formed from crossed SWNTs or small bundles (< 3 nm) have shown that semiconducting-semiconducting and metallic-metallic SWNT junctions form excellent tunneling contacts despite the small contact area and that such junctions have high conductivities, whereas semiconducting-metallic SWNTs form a Schottky barrier with a height approximately equal to half the band gap of the semiconducting SWNT.³⁶

Figure 5 shows the temperature dependence of the conductivity of the SWNT films. The resistance of films with a thickness of ≈ 1 nm was found to increase by 3-4 orders of magnitude

(34) Stauffer, D. *Introduction to Percolation Theory*; Taylor & Francis: London and Philadelphia, 1985.

(35) Sahimi, M. *Applications of Percolation Theory*; Taylor & Francis: London, 1994.

(36) Fuhrer, M. S.; Nygard, J.; Shih, L.; Forero, M.; Yoon, Y.-G.; Mazzone, M. S. C.; Choi, H. J.; Ihm, J.; Louie, S. G.; Zettl, A.; McEuen, P. L. *Science* **2000**, 288, 494-497.

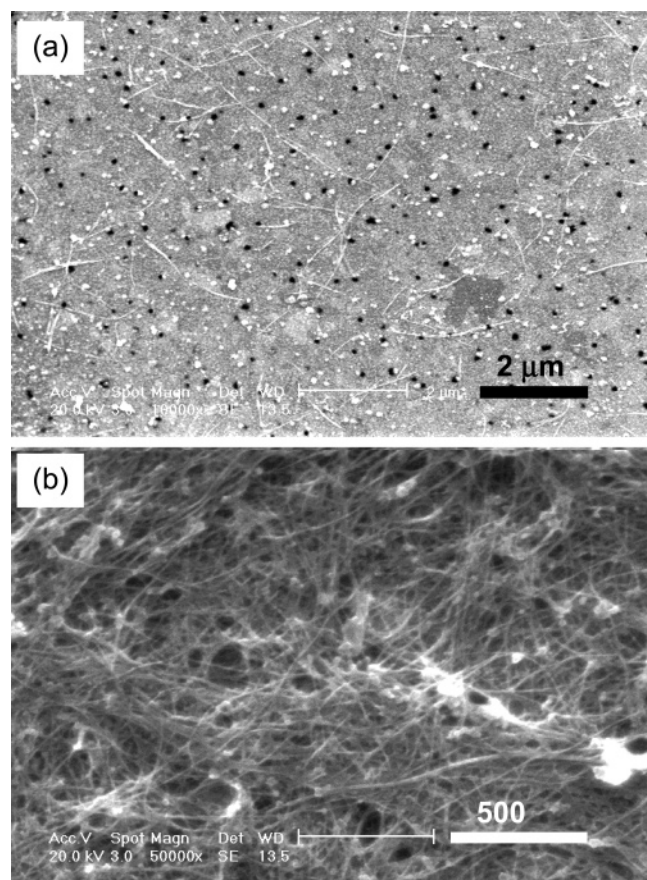


Figure 4. SEM micrographs of networks of low and high interconnectivity: (a) P2-SWNT thin film ($t < t_c$) and (b) P3-SWNT thick film ($t > t_c$). The micrographs were recorded on a Philips XL30-FEG scanning electron microscope. The black dots in (a) are from the substrate.

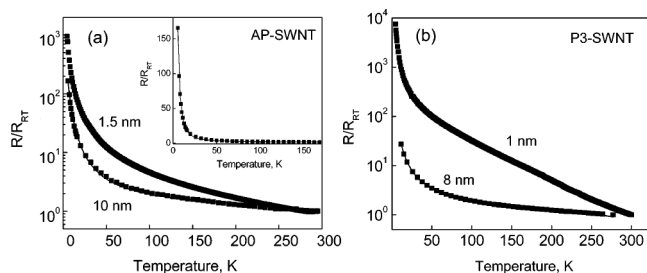


Figure 5. Temperature dependence of the normalized resistance of films of various thicknesses: (a) AP-SWNT and (b) P3-SWNT. Equation 2 was fit to the data for the 10 nm AP-SWNT and 8 nm P3-SWNT films; the inset in (a) shows the fit on a linear scale. The fitting line is not visible in (b), as it falls under the experimental points throughout the whole temperature range (some of the experimental points are omitted for clarity).

as the temperature was lowered from room temperature to 4 K, whereas films 10 nm in thickness showed an increase of resistance by no more than 2 orders of magnitude. The large increase in resistance with decreasing temperature observed in the films is not an intrinsic property of individual SWNTs; the conductivity of a SWNT rope has been reported to change by a factor of < 4 over the same temperature range.^{24,37} It appears likely that the conductivity of the SWNT networks is limited by thermally assisted tunneling at the intertube junctions, which is necessary for the passage of a current, and therefore the network properties are a strong function of the film thickness

(and connectivity). The weaker temperature dependence of thicker films suggests an increase in the concentration of efficient (low resistance) intertube contacts as the film thickness is increased in accord with the percolation model presented above.

To further characterize the electronic transport properties and the mechanism of conduction in the SWNT networks, we analyzed the temperature dependence of the resistance of thick films. The films show negative dR/dT between 4 and 300 K, indicative of nonmetallic behavior. Ropes of SWNTs²⁴ and mats of SWNTs^{24,38,39} typically exhibit metallic behavior over a relatively wide temperature range, which changes to nonmetallic behavior at low temperatures with a crossover temperature, T^* , between 35 and 220 K. However, for mats of electric arc produced carbon nanotubes a crossover to metallic behavior is not observed up to 300 K, and it has been argued that T^* shifts to higher temperature as a result of high intertubular coupling.²⁵

The mixed metallic- nonmetallic character in the conductivity of SWNTs has been attributed to series conduction between metallic islands that is interrupted by small tunneling barriers (eq 2).²⁶

$$F(T) = \frac{1}{\hat{\chi}(T)} = A \exp\left(-\frac{T_m}{T}\right) + B \exp\left(-\frac{T_b}{T_s + T}\right) \quad (2)$$

The first term in eq 2 accounts for the quasi-1-D metallic conduction with a characteristic energy $k_b T_m$ to account for the backscattering of the charge carriers, and the second term corresponds to fluctuation-induced tunneling between metallic regions that are separated by small barriers; A and B are geometrical factors, $k_b T_b$ is the energy required for charge carrier tunneling through the barriers, and T_s/T_b is the quantum-induced tunneling in the absence of fluctuations and accounts for the suppression of the conductivity at low temperature.

We were able to fit the data without the necessity of including the metallic term in eq 2; small deviations of the theoretically derived curve are apparent in the AP-SWNT data at temperatures higher than 200 K. We obtained values of $T_b = 79$ K (6.8 meV) and 84 K (7.2 meV) for AP-SWNT and P3-SWNT films, respectively, indicative of small tunneling barriers between the metallic regions. These values of T_b are of the same order of magnitude as those found for carbon nanotube ropes with tangled regions (65 K)²⁶ and for mats of SWNTs (100 K).⁴⁰ The values for the ratio T_s/T_b are 0.13 and 0.15 for AP-SWNT and P3-SWNT, respectively. The excellent fits to the experimental data suggest that the carrier transport in the SWNT films is consistent with a model of tunneling through small barriers between conducting islands.

Electronic Properties of Functionalized SWNT Networks.

Modification of the electronic structure of SWNTs by chemical functionalization has been demonstrated to provide a valuable route for the development of advanced sensor materials.¹⁷ To understand the effect of chemical modification on the electronic properties of functionalized nanotubes, we have studied networks of SWNTs functionalized with octadecylamine (ODA)⁴¹ and poly(*m*-aminobenzene sulfonic acid) (PABS).⁴² ODA is an insulating organic molecule, whereas PABS is a self-doped water-soluble conducting polymer;⁴³⁻⁴⁷ both functionalization

(37) Lee, R. S.; Kim, H. J.; Fischer, J. E.; Lefebvre, J.; Radosavljevic, M.; Hone, J.; Johnson, A. T. *Phys. Rev. B* **2000**, *61*, 4526-4529.

(38) Grigorian, L.; Williams, K. A.; Fang, S.; Sumansekera, G. U.; Loper, A. L.; Dickey, E. C.; Pennycook, S. J.; Eklund, P. C. *Phys. Rev. Lett.* **1998**, *80*, 5560-5563.
(39) Fuhrer, M. S.; Cohen, M. L.; Zettl, A.; Crespi, V. H. *Solid State Commun.* **1999**, *109*, 105-109.
(40) Kaiser, A. B.; McIntosh, G. C.; Edgar, K.; Spencer, J. L.; Yu, H. Y.; Park, Y. W. *Curr. Appl. Phys.* **2001**, *1*, 50-55.

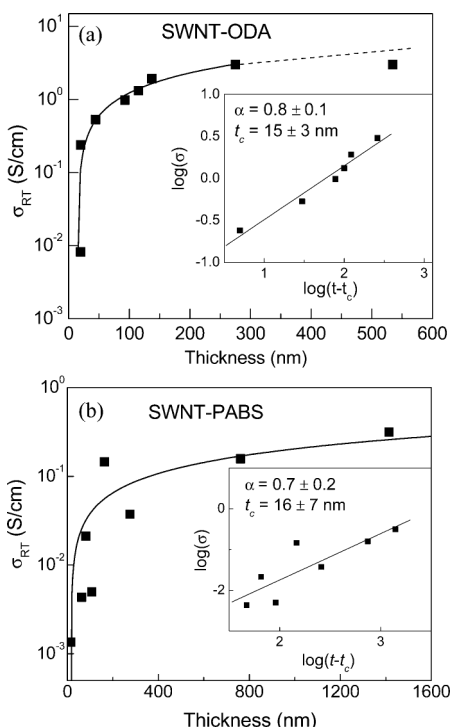
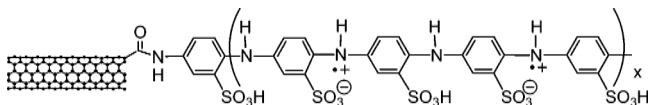


Figure 6. Conductivity of films of (a) SWNT-ODA and (b) SWNT-PABS. The solid lines are fits of the experimental data to the power scaling equation $\hat{\sigma}_{RT} \propto (t - t_c)^{\alpha}$. The insets show the conductivity, $\hat{\sigma}_{RT}$, as a function of $(t - t_c)$ on a logarithmic scale.

Scheme 1. Chemical Structure of PABS-Functionalized SWNT



schemes make use of the carboxylic acid functionalities introduced during purification with nitric acid, which have been shown to leave the sidewalls and the electronic structure of the SWNTs largely intact.⁴⁸

The functionalization of SWNTs with ODA renders them soluble in common organic solvents,⁴¹ and it has been shown that the amount of the attached ODA moieties in the compound corresponds to 50 wt %.⁴⁹ On the basis of the large fraction of attached functional groups, the functionalization has been suggested to occur at impurities as well as the ends and defect sites of the SWNTs.

The films of SWNT-ODA show conductivities that are about 2 orders of magnitude lower than those of the nonfunctionalized SWNTs. Films of thickness above 100 nm exhibit a room-temperature conductivity of ≈ 3 S/cm (Figure 6a). The percolation threshold of the films is 15 nm, and it seems likely that

the lower conductivity and higher percolation threshold of the films are due to the introduction of increased tunneling barriers between the functionalized SWNTs due to the steric bulk afforded by the substituents. From the standpoint of percolation theory, the introduction of the insulating substituents works to dilute the concentration of the conducting pathways.

Even lower conductivities are observed for films of SWNT-PABS (Figure 6b). The conductivity of thick films (> 100 nm) is ≈ 0.3 S/cm, an order of magnitude lower than the conductivity of SWNT-ODA films, but higher than values found for pressed pellets of SWNT-PABS ($\hat{\sigma}_{RT} \approx 5.6 \times 10^{-3}$ S/cm).⁴²

In contrast to the functionalization with ODA, covalent bonding of PABS to SWNTs alters the electronic structure of SWNTs. The absorption spectra of SWNT-PABS suggest that there is an electronic interaction between the SWNT and PABS functionalities.⁴² The strong electron-withdrawing nature of the iminium cations and the sulfonic acid groups present in the parent structure of PABS (Scheme 1)¹⁷ may be responsible for extracting electrons from the metallic SWNTs, localizing some of the conduction electrons, and thus lowering the effectiveness of the conducting channels as well as introducing additional tunneling barriers in the network. In fact SWNT-PABS networks are more sensitive to the presence of ammonia than unfunctionalized SWNTs,¹⁷ and this may be due to the fact that the PABS functionality is able to introduce a small fraction of holes into the conduction band of the semiconducting SWNTs, which become compensated in the presence of ammonia.

While the thick-film conductivities differ by an order of magnitude, the SWNT-ODA and SWNT-PABS films both give a percolation threshold of ≈ 15 nm (Figure 6). The higher percolation threshold in these materials reflects the dilution of the SWNTs, which provides the conducting pathway (for neat PABS, $\hat{\sigma}_{RT} \approx 5 \times 10^{-5}$ S/cm).^{46,47}

Conclusions

The room-temperature conductivities of as-prepared and purified SWNTs in the thick film limit are in the range 250–400 S/cm. The relatively low conductivity compared to individual SWNTs and the strong temperature dependence of the conductivity indicate the presence of tunneling barriers, which dominate the overall film conductivity. The films are nonmetallic in the temperature range 4–300 K and behave as percolating networks with a power law dependence of the conductivity on the film thickness and show quasi-two-dimensional charge transport. The percolation threshold occurs in the vicinity of one monolayer bundle of SWNTs. Chemical functionalization decreases the conductivity of the films by 2 or 3 orders of magnitude and increases the percolation threshold by a factor of 5, in accord with the previous finding that chemical functionalization amplifies the ability of SWNTs to interact with specific chemical species and has implications for further development of analyte-specific sensor devices.

Acknowledgment. This research was supported by DOD/DARPA/DMEA (Award No. DMEA90-02-2-0216). Work at Carbon Solutions, Inc. was performed under a subcontract from Smiths Detection-Pasadena, CA, under HSARPA award (RA0103-20030923). We are grateful to the referees for a number of helpful suggestions.

Supporting Information Available: AFM data and absorption spectra of SWNT films as a function of thickness. This material is available free of charge via the Internet at <http://pubs.acs.org>. JA043153L

- (41) Chen, J.; Hamon, M. A.; Hu, H.; Chen, Y.; Rao, A. M.; Eklund, P. C.; Haddon, R. C. *Science* **1998**, *282*, 95–98.
- (42) Zhao, B.; Hu, H.; Haddon, R. C. *Adv. Func. Mater.* **2004**, *14*, 71–76.
- (43) Cao, Y.; Andreatta, A.; Heeger, A. J.; Smith, P. *Polymer* **1989**, *30*, 2305.
- (44) Wei, X. L.; Wang, Y. Z.; Long, S. M.; Bobeczko, C.; Epstein, A. J. *J. Am. Chem. Soc.* **1996**, *118*, 2545–2555.
- (45) Ito, S.; Murata, K.; Teshima, S.; Aizawa, R.; Asako, Y.; Takahashi, K.; Hoffman, B. M. *Synth. Met.* **1998**, *96*, 161–163.
- (46) Roy, B. C.; Gupta, M. D.; Bhowmik, L.; Ray, J. K. *Synth. Met.* **1999**, *100*, 233–236.
- (47) Roy, B. C.; Gupta, M. D.; Bhowmik, L.; Ray, J. K. *Synth. Met.* **2002**, *130*, 27–33.
- (48) Niyogi, S.; Hamon, M. A.; Hu, H.; Zhao, B.; Bhowmik, P.; Sen, R.; Itkis, M. E.; Haddon, R. C. *Acc. Chem. Res.* **2002**, *35*, 1105–1113.
- (49) Hamon, M. A.; Hu, H.; Bhowmik, P.; Niyogi, S.; Zhao, B.; Itkis, M. E.; Haddon, R. C. *Chem. Phys. Lett.* **2001**, *347*, 8–12.